Soft Matter

RSC Publishing

PAPER

Unravelling the behaviour of curcumin nanoemulsions during *in vitro* digestion: effect of the surface charge

Cite this: *Soft Matter*, 2013, **9**, 3147

Ana C. Pinheiro,[a] Mita Lad,[b] Hélder D. Silva,[a] Manuel A. Coimbra,[c] Michael Boland[b] and António A. Vicente*[a]

Oil-in-water nanoemulsions containing curcumin were prepared through high-pressure homogenization using corn oil and three different emulsifiers: Tween 20 (non-ionic), Sodium Dodecyl Sulphate (SDS, anionic) and DodecylTrimethylAmmonium Bromide (DTAB, cationic). A human gastric simulator was used as the *in vitro* digestion model (in which the stomach, duodenum, jejunum and ileum steps were performed) to evaluate the impact of surface charge on the digestion of the curcumin nanoemulsions. This model allowed the simulation of continuous peristaltic movements and consequently enabled a more mechanically realistic simulation of the dynamic digestion process than simple stirred vessel models. The emulsifier charge had a significant effect on the droplet size, particle electric charge and microstructure of curcumin nanoemulsions during the simulated digestion, which consequently influenced the free fatty acid release and curcumin bioavailability. The results showed the positively charged DTAB-stabilized emulsions to be the least stable during the digestion process, exhibiting the largest increase in droplet size and eventual phase separation. This also contributed to the low bioavailability of curcumin. Conversely, emulsions stabilized with Tween 20 showed retention of emulsion structure (high surface area) and greater free fatty acid production, which could explain the increased curcumin bioavailability. The emulsifier charge influenced the lipid digestion process and the bioavailability of the bioactive compound incorporated, probably by altering the ability of bile salts and digestive enzymes to adsorb onto the emulsion surfaces, thus altering the droplet size (and consequently the surface area) due to droplet breakup or coalescence within the digestive tract. The results of this work also highlighted the importance of subjecting the emulsions to a simulated gastric environment, since changes in pH, ionic strength, gastric enzyme activity and shear will impact the emulsion properties in the small-intestine. This manuscript has provided important insights into the effect of emulsifier charge on the behaviour of nanoemulsions during *in vitro* digestion, which is important to determine their functional performance, aiming at the optimization of nanoemulsion-based delivery systems to protect and release bioactive lipophilic compounds.

Received 2nd November 2012
Accepted 14th January 2013

DOI: 10.1039/c3sm27527b

www.rsc.org/softmatter

1 Introduction

Curcumin is a yellow pigment derived from the rhizomes of the *Curcuma longa* (commonly known as turmeric). This natural polyphenol is an important natural colorant used in food[1] and has gained considerable attention in recent years due to its wide range of biological activities, such as anti-oxidant,[2] anti-microbial,[3] anti-inflammatory,[4] wound healing[5] and anti-tumoral effects.[6] However, the applicability of curcumin as a health-promoting agent is limited by its poor solubility in aqueous solution and its low bioavailability. The reduced bioavailability of curcumin is related to its poor absorption, rapid metabolism and rapid systemic elimination.[7] The bioavailability of poorly water-soluble compounds such as curcumin can be greatly enhanced by incorporating them into emulsion-based delivery systems. An oil-in-water emulsion can be produced by homogenizing the oil phase containing the lipophilic bioactive compound with an aqueous phase containing a water-soluble emulsifier.[8] Emulsions can have a wide range of droplet sizes, depending on the composition of the system and on the method of homogenization used. Emulsions formed on the nanometer scale have better stability against droplet aggregation as the attractive forces acting between the droplets decreases with decreasing particle size. The bioavailability of encapsulated lipophilic components within the gastrointestinal tract may, in principle, be increased by using nanoemulsions due to the small particle size and high surface-to-volume ratio.[9]

[a]*IBB – Institute for Biotechnology and Bioengineering, Centre of Biological Engineering, University of Minho, Campus de Gualtar, 4710-057 Braga, Portugal. E-mail: avicente@deb.uminho.pt; Fax: +351 253 678986; Tel: +351 253 604419*

[b]*Riddet Institute, Massey University, Private Bag 11 222, Palmerston North 4442, New Zealand*

[c]*QOPNA, Department of Chemistry, University of Aveiro, 3810-193 Aveiro, Portugal*

In humans, the hydrolysis of lipids starts in the stomach (pH 1 to 3) by the action of gastric lipase, which hydrolyses about 10 to 30% of the ingested triacylglycerols, generating mainly free fatty acids and diacylglycerols. This facilitates the subsequent lipid hydrolysis in the duodenum by pancreatic lipase by allowing fat emulsification and promoting enzyme activity.[10] The encapsulated lipophilic bioactive compound is released upon digestion of the emulsion and is incorporated into the bile salt/phospholipid micelles (mixed micelles) and then transported through the mucous layer to the surfaces of the enterocytes where it is absorbed.[11] The formation of mixed micelles facilitates the molecular absorption of lipophilic compounds from the small intestine into the bloodstream.[12]

In recent years, different *in vitro* digestion models have been developed as a means for understanding the physicochemical processes associated with the digestion process. The pH-stat method is a simple *in vitro* lipolysis model commonly used to characterize the lipid digestion under simulated small intestinal conditions. This method allows the measurement of the free fatty acids (FFA) released from triacylglycerols over time and can be used to rapidly evaluate the impact of different formulations or conditions on lipid digestion.[13] Some of the complex dynamic gastrointestinal models include the dynamic gastric model (DGM), which was designed to replicate the real-time changes in pH, enzyme addition, shearing, mixing and retention time of an adult human stomach,[14] the TIM model, which simulates the physiological conditions of the human stomach and small intestine,[15] and the Human Gastric Simulator (HGS), a model that allows for the simulation of the continuous peristaltic movements of stomach walls with similar amplitude and frequency of contraction forces as reported *in vivo*.[16] This model also incorporates gastric secretion, emptying systems and temperature control that enable a more realistic simulation of the dynamic digestion process.

Most of the works that evaluate the behaviour of emulsions during digestion use simple *in vitro* models that do not include a gastric stage.[17–19] The passage of nanoemulsions through the highly acidic conditions in the stomach involves physical destabilization of emulsions, once the composition, size and interfacial characteristics of the lipid droplets are altered.[20] Therefore, more realistic *in vitro* digestion models should be used.

The emulsifier type will impact the susceptibility of the lipid droplets to coalescence and break up within the gastrointestinal (GI) tract, thereby altering the total surface area of lipid exposed to lipase absorption and activity.[21] The characteristics of the interfacial layer surrounding the lipid droplets will influence the ability of lipase to interact with the lipid phase, and consequently, the rate of lipid digestion.

In the present work, the human gastric simulator model was used to mimic the mechanical and chemical environments of the human stomach, duodenum, jejunum and ileum. The impact of the emulsifier type on the structural changes of curcumin nanoemulsions and on curcumin bioavailability during *in vitro* digestion was evaluated. In particular, the impact of emulsifier charge was evaluated using Tween 20 (non-ionic), sodium dodecyl sulphate (SDS, anionic) and dodecyltrimethylammonium bromide (DTAB, cationic) as emulsifiers.

2 Experimental

2.1 Materials

Corn oil was purchased from a local supermarket in Palmerston North (New Zealand) and was used without further purification. Curcumin, Tween 20 and sodium dodecyl sulphate (SDS) were purchased from Sigma-Aldrich (St Louis, MO) and dodecyltrimethylammonium bromide (DTAB) was acquired from Acros Organics. Pepsin from porcine gastric mucosa, amano lipase A from *Aspergillus niger*, pancreatin from porcine pancreas (8 × USP), bile extract porcine and the salts used for preparing the gastric electrolyte solution and the small intestinal electrolyte solution, hydrochloric acid and sodium bicarbonate were purchased from Sigma-Aldrich (St Louis, MO). Chloroform was obtained from BDH chemicals (Poole, England).

Milli-Q water (water purified by treatment with Milli-Q apparatus, Millipore Corp., Bedford, MA, USA) was used to prepare all solutions.

2.2 Emulsion preparation

The curcumin nanoemulsions were prepared by homogenizing 5 wt% corn oil containing 0.1 wt% of curcumin with 95 wt% aqueous emulsifier solution (0.5 wt% Tween 20, SDS or DTAB), using a high-speed blender for 2 min followed by passage through a microfluidizer (Microfluidics M-110P) at 20 000 psi (137.9 MPa), for 5 cycles.

2.3 *In vitro* digestion

In vitro digestion was performed by simulating the gastric, duodenal, jejunal and ileal portions of the GI tract as described by other authors[15] with the following modifications. A volume of 300 ml of curcumin nanoemulsions with the selected emulsifier was introduced into the human gastric simulator and the experiment was run for a total of 5 h, simulating the average physiological conditions of the gastrointestinal tract by the continuous addition of gastric, duodenal, jejunal and ileal secretions. The gastric secretion consisted of pepsin and lipase in a gastric electrolyte solution (NaCl 4.8 g l^{-1}, KCl 2.2 g l^{-1}, $CaCl_2$ 0.22 g l^{-1} and $NaHCO_3$ 1.5 g l^{-1}), secreted at a flow rate of 0.5 ml min^{-1}. The pH was controlled to follow a predetermined curve (from 4.8 at $t = 0$ to 1.7 at $t = 120$ min) by secreting hydrochloric acid (1 M). The duodenal secretion consisted of a mixture of 30 ml of 4% (w/v) porcine bile extract, 15 ml of 7% (w/v) pancreatin solution and 9 ml of a small intestinal electrolyte solution (SIES) (NaCl 5 g l^{-1}, KCl 0.6 g l^{-1}, $CaCl_2$ 0.25 g l^{-1}) at a flow rate of 0.9 ml min^{-1}. The jejunal secretion fluid consisted of SIES containing 10% (v/v) porcine bile extract solution at a flow rate of 3.2 ml min^{-1}. The ileal secretion fluid consisted of SIES at a flow rate of 3.0 ml min^{-1}. The pH in the different parts of small intestine was controlled by the addition of 1 M sodium bicarbonate solutions to set-points of 6.5, 6.8 and 7.2 for simulated duodenum, jejunum and ileum, respectively.

2.4 Particle size

The particle size of the emulsions was measured at different stages of digestion by both dynamic light scattering (Zetasizer Nano ZS, Malvern Instruments, Worcestershire, UK) and static light scattering (Mastersizer 2000 Hydro MU, Malvern Instruments Ltd, Malvern, Worcestershire, UK).

The *z*-average mean diameter was calculated by the Zetasizer instrument using the Stokes–Einstein equation, assuming that the nanoemulsion droplets were spherical. Before measurement, the samples were diluted at a ratio of 1 : 100 (v/v) in an appropriate buffer solution with the same pH as the aqueous phase of the sample (citrate buffer (10 mM, pH 2) for stomach step and phosphate buffer (10 mM, pH 7) for before digestion and small intestine steps[21]) at room temperature to avoid multiple scattering effects. The measurements were performed at least in triplicate.

The particle size distribution was also measured by the Mastersizer instrument, which measures the angular dependence of the intensity of laser light scattered by a dilute emulsion and then finds the particle size distribution that gives the best fit between the experimental measurements and predictions made using light-scattering theory (Mie theory). To avoid multiple scattering effects the emulsions were diluted in distilled water at a ratio of 1 : 100 (v/v).

Data fitting – particle size distribution ($d4,3 = (\sum n_i d_i 4/\sum n_i d_i 3)$ where n_i is the number of droplets of diameter d_i) of the emulsions was recorded before and during simulated digestion using refractive indices of 1.47 and 1.33 for droplet and dispersed (water) phase respectively.

2.5 ζ-Potential

The ζ-potential values of nanoemulsions at different stages of digestion were measured using a particle electrophoresis instrument (Malvern Instruments, Worcestershire, UK). The ζ-potential was determined by measuring the direction and velocity of droplet movement in the applied electric field and was calculated by the instrument using the Smoluchowski model.

The samples were diluted 100 times in appropriate buffer solution (citrate buffer (10 mM, pH 2) for the stomach step and phosphate buffer (10 mM, pH 7) for before digestion and small intestine steps[21]) at room temperature before measurement and each individual ζ-potential measurement was determined from the average of three readings.

2.6 Confocal microscopy

The microstructure of the oil droplets in the emulsion was studied using a confocal scanning laser microscope (Leica TCS SP5 DM6000B, Heidelberg, Germany) with an ×100 oil immersion objective lens. Samples were stained with Nile Red (9-diethylamino-5*H*-benzo[α]phenoxazine-5-one, 0.25 mg ml^{-1} in dimethyl sulfoxide, 1 : 10 (dye:sample), v/v), which enabled the oil droplets to become visible. Slides were prepared by taking a portion of the stained emulsion solution and placing in a concave glass microscope slide and covering with a glass cover slip.

2.7 Free fatty acid release

A measure of lipolysis is the production of free fatty acids (FFA) with increased digestion time, which leads to a decrease in the pH of the system. A pH-stat automatic titration unit (TIM 856 titration manager, Titralab, Radiometer analytical) was used to automatically monitor the pH and maintain it at a pre-set value by titrating with 0.05 M NaOH solution. The volume of NaOH added to the emulsion was recorded, and used to calculate the concentration of FFA generated by lipolysis.

A sample of emulsion was collected from the HGS after 120 min (after stomach simulation) and diluted in an appropriate quantity of small intestinal electrolyte solution (SIES), to obtain the same emulsion concentration as in the HGS at the end of digestion. Then pancreatin and bile extract were added and back titration was used to measure the total free fatty acids. After incubation of the emulsions at pH 7.0 for a certain period of time, the pH was rapidly increased with NaOH to pH 9.0 to stop the reaction and to favour the release of FFA. Therefore, the total FFA was assessed by titration, measuring the volume necessary to reach pH 9.0.[22] Back titration was performed at pH 9.0 in order to ensure full ionization and titration of free fatty acids.[23]

Blank experiments (without pancreatin) were performed in order to determine the volume of NaOH required to raise the pH to 9.0. This was required for the calculation of total free fatty acids liberated according to eqn (1). The quantity of fatty acids liberated was calculated based on the following equation:[24]

$$\frac{\mu\text{mol}_{\text{fatty acid}}}{\text{ml}_{\text{sample}}} = \frac{\left(\text{volume}_{\text{NaOH for sample}} - \text{volume}_{\text{NaOH for blank}}\right) \times C \times 1000}{\text{volume}_{\text{sample}}} \quad (1)$$

where C is the molar concentration of the NaOH titrant used (0.05 in this case).

2.8 Curcumin bioavailability

It was assumed that the fraction of the original curcumin that ended up in the micelle phase was a measure of curcumin bioavailability.[8] Therefore, the curcumin bioavailability at different stages of digestion was determined based on the methodology described by other authors.[8] Briefly, 10 ml of the emulsions were centrifuged (Sorvall evolution RC. Thermo Scientific) (18 675*g*) at room temperature for 30 min. The micelle phase (5 ml) was collected, vortexed with 5 ml of chloroform, and then centrifuged at 651*g*, at room temperature, for 10 min. The bottom chloroform layer was collected and the extraction procedure was repeated with the top layer. The second bottom chloroform layer was added to the previously set aside chloroform layer, mixed, and analysed by UV-VIS spectrophotometer (Genesys 10uV, Thermo Scientific) at 422 nm (absorbance peak). The concentration of curcumin was

determined from a previously prepared calibration curve of absorbance *versus* curcumin concentration in chloroform.

2.9 Statistical analysis

All experiments were carried out in triplicate using freshly prepared samples. The results were then reported as averages and standard deviations of these measurements. The statistical analyses were carried out using analysis of variance, Tukey's mean comparison test ($p < 0.05$) and linear regression analysis (SigmaStat, trial version, 2003, USA).

3 Results and discussion

3.1 Influence of digestion on particle size

Initially, we characterized the change in particle size distribution of the nanoemulsions as a function of digestion time. Fig. 1 shows the mean hydrodynamic diameter of curcumin nanoemulsions at different stages of the simulated digestion process namely initial (before digestion), stomach, duodenum, jejunum and ileum, determined using a dynamic light scattering methodology.

All the emulsifiers tested formed stable nanoemulsions with *z*-average diameters of 124.2 ± 8.4, 152.9 ± 2.2 and 119.5 ± 4.5 nm, for Tween 20, SDS and DTAB stabilized nanoemulsions, respectively. The monodispersity of the nanoemulsions can be evaluated by its polydispersity index (PDI), which can range from 0 to 1 (with 0 being monodisperse and 1 being polydisperse). The nanoemulsions stabilized by SDS and DTAB exhibit a narrow size distribution (PDI = 0.19 ± 0.02 and 0.22 ± 0.01, respectively), whereas the Tween 20 stabilised emulsions present a lower monodispersity (PDI = 0.42 ± 0.03).

During the simulated digestion, all nanoemulsions showed an increase in size, although the precise mechanism was not identified. The increase in droplet size observed could be attributed to aggregation, coalescence or flocculation due to the action of digestive enzymes as well as changes in pH and ionic strength. From the data presented it would appear that emulsions stabilized with DTAB were the least stable, showing the greatest increase in particle diameter ($p < 0.05$).

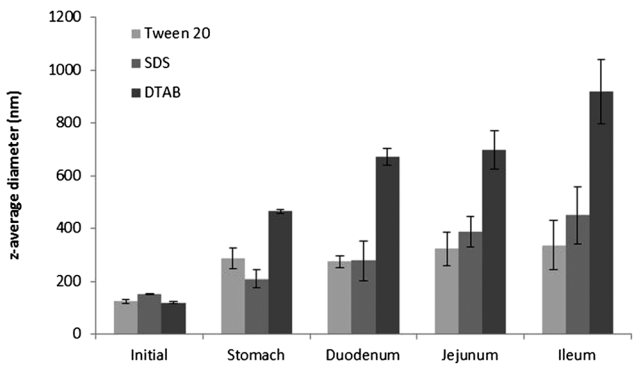

Fig. 1 Dynamic light scattering-based mean particle diameter of curcumin nanoemulsions stabilized by different emulsifiers (Tween 20, SDS and DTAB) as they pass through an *in vitro* digestion model.

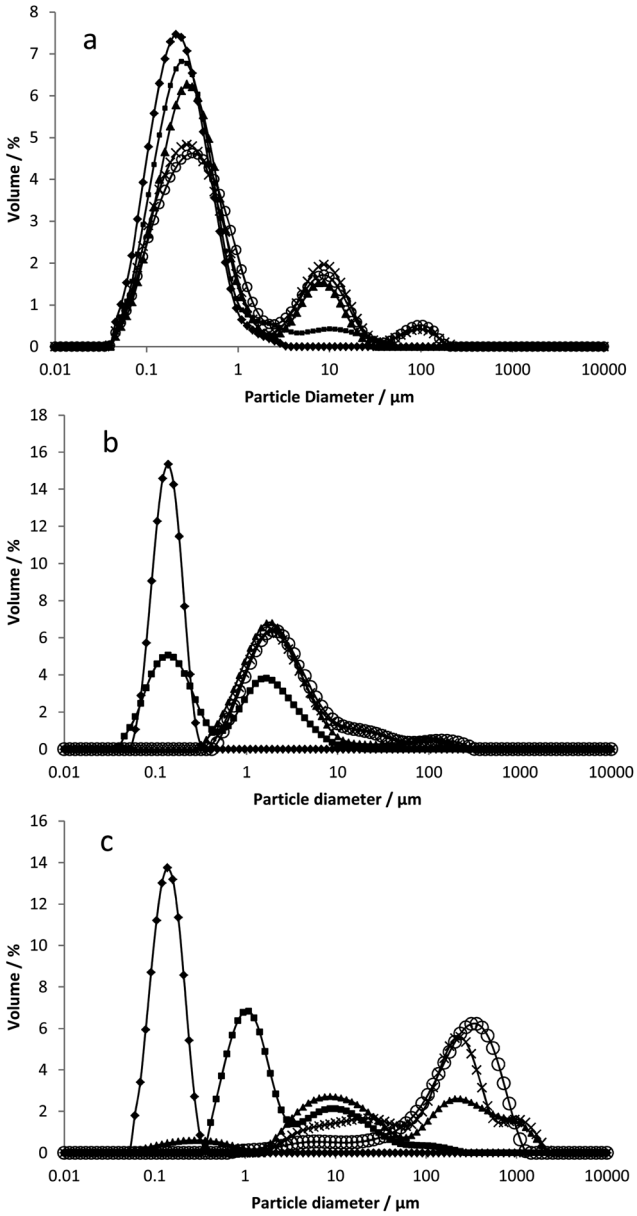

Fig. 2 Static laser light scattering-based particle size distribution curves of curcumin nanoemulsions stabilized by different emulsifiers: Tween 20 (a); SDS (b) and DTAB (c). Each stage of *in vitro* digestion is represented as follows; initial (◆), stomach (■), duodenum (▲), jejunum (×) and ileum (○).

It should be noted that dynamic light scattering has a size limitation: it is suitable for the measurement of particle diameters up to few microns (≤10 μm). Therefore, to detect the extent to which the emulsion drop diameter had increased, the emulsions were also analysed using static light scattering (Fig. 2).

The droplet size distribution of the emulsions obtained using static light scattering showed that the initial nanoemulsions had a monomodal size distribution for all emulsifier types. For Tween 20 nanoemulsions (Fig. 2a), after the addition of simulated gastric fluids, the emulsions started to show a bimodal distribution, with a second peak in the region of 10 μm and a corresponding decrease in the area of the first peak. The

addition of simulated intestinal fluids resulted in a multimodal distribution, with a third peak appearing in the range of 100 μm, and a gradual decrease of the initial peak (centred ~ 0.1 μm). This result suggests that the change in size distribution was an effect of digestive enzymes and not an effect of the change in pH, ionic strength or shear, as there was no change in the size distribution for the control experiment performed with everything but the enzyme (data not shown). In the case of SDS nanoemulsions (Fig. 2b), a more rapid decrease in the nanometer size emulsion droplets was observed and a new population of relatively large particles (around 1 μm) was formed as the emulsions passed through the *in vitro* system. For DTAB-stabilized emulsions (Fig. 2c), the nanometer-range peak disappeared and the distribution became multimodal when the nanoemulsions were subjected to simulated gastric conditions. Under simulated intestinal conditions, the droplet sizes increased further, reaching approximately 1000 μm. For nanoemulsions stabilized with both SDS and DTAB, there was a significant decrease in droplets in the nanometer size range, especially under simulated gastric conditions. The increase in droplet size and the presence of a multimodal size distribution cannot be simply explained by the activation or presence of the digestion enzymes. Our control results (without enzymes – data not shown) also showed an increase in droplet diameter with digestion time suggesting that the change in pH, ionic strength and shear contribute to weakening of the emulsion interface promoting coalescence of the oil drops. In the case of DTAB this interfacial weakening could result from the strong binding of bile salts (an interaction promoted by the strong electrostatic binding), which are known to displace emulsifiers at the emulsions interface, facilitating the binding of lipase and thus enabling lipolysis.[21] According to other authors, emulsions stabilized by non-ionic surfactants (such as Tween 20) are more stable in the acidic gastric environment due to steric repulsion provided by the polyoxyethylene head group.[25]

The results obtained by static light scattering (Mastersizer) are in agreement with the trend observed for the dynamic light scattering (Zetasizer). However, in general, the hydrodynamic diameters measured by Zetasizer are lower than those measured by Mastersizer, which may be explained by the fact that the larger coalesced droplets rapidly creamed to the top of the Zetasizer cell and thus escaped to the detection by the laser and the detection beam passed through an unrepresentative fraction of emulsions containing relatively small droplets.[26]

These results show that the nature and extent of the changes in lipid droplet size as the emulsions pass through an *in vitro* digestion model depends on the emulsifier type, confirming the results of previous work.[14,21] This work, however, also brings new insight in suggesting that is a contribution made by changes in pH, ionic strength and shear and highlights the importance of subjecting the emulsion to the simulated gastric environment.

3.2 Influence of digestion on emulsion microstructure

The microstructure of the curcumin nanoemulsions stabilized by different emulsifiers at each stage of the simulated digestion was determined by confocal microscopy (Fig. 3a). Due to the size of the emulsion droplets (nm) before digestion, Brownian motion prevents the droplets from being clearly visible. However, with digestion time the size of the droplets increases thus enabling them to be clearly detected under the confocal microscope.

The microscopy images show that before digestion, the nanoemulsions stabilised by Tween 20 contain a greater population of larger droplets compared with the other initial nanoemulsions, which is in accordance with its higher PDI value. All curcumin nanoemulsions present a spherical morphology and during the simulated digestion, a significant increase in nanoemulsion particle size was observed, showing the same tendency obtained with the size results. As demonstrated with the particle size data in Fig. 2, the confocal images show that as *in vitro* digestion progresses, emulsions stabilized with Tween 20 appear to have a larger droplet size when compared to emulsions formed with SDS. This however, is much smaller than the oil droplet size visible after 120 min of simulated gastric digestion for the emulsion formed with DTAB. The confocal images for the later stages of the simulated digestion of the DTAB emulsion also show a reduction in the amount of oil drops present. Our explanation for this observation is that this particular emulsion was highly unstable, leading to eventual phase separation (Fig. 3b). Therefore, the confocal images of DTAB-stabilized emulsions from the simulated intestinal stage show small lipid droplets remaining in the water phase. Our confocal images, in general, suggest a coalescence-based mechanism for the increase in emulsion drop diameter. There also appears to be possible clustering of emulsion drops of the emulsion stabilized with Tween 20 in the ileum.

These results suggest that the stability of nanoemulsions to coalescence during digestion is strongly affected by the initial emulsifier. The emulsifier type influences the ability of lipase to come in contact with the emulsified lipid, and this, together with the production of free fatty acids (FFA), monoacylglycerols (MAG) and diacylgycerides (DAG) at the droplet surfaces during lipid digestion will modify the emulsion interface. These surface-active products of digestion are ineffective at stabilizing oil-in-water emulsions against coalescence.[26] This could explain the observed changes in emulsion structure as digestion progressed through the simulated GI tract.

3.3 Influence of digestion on droplet charge

The surface electrical charge (ζ-potential) of the curcumin nanoemulsions as they passed through the different stages of the *in vitro* digestion model provides information about changes in interfacial composition (Fig. 4).

The ζ-potential of the initial nanoemulsions stabilized by Tween 20, SDS and DTAB was -1.03 ± 0.64, -92.86 ± 5.89 and 89.42 ± 7.18 mV, respectively. These electrical charges are to be expected as Tween 20, SDS and DTAB are non-ionic, anionic and cationic emulsifiers, respectively.

Under simulated gastric conditions, there was no significant ($p > 0.05$) change in the ζ-potential for the Tween 20 and DTAB

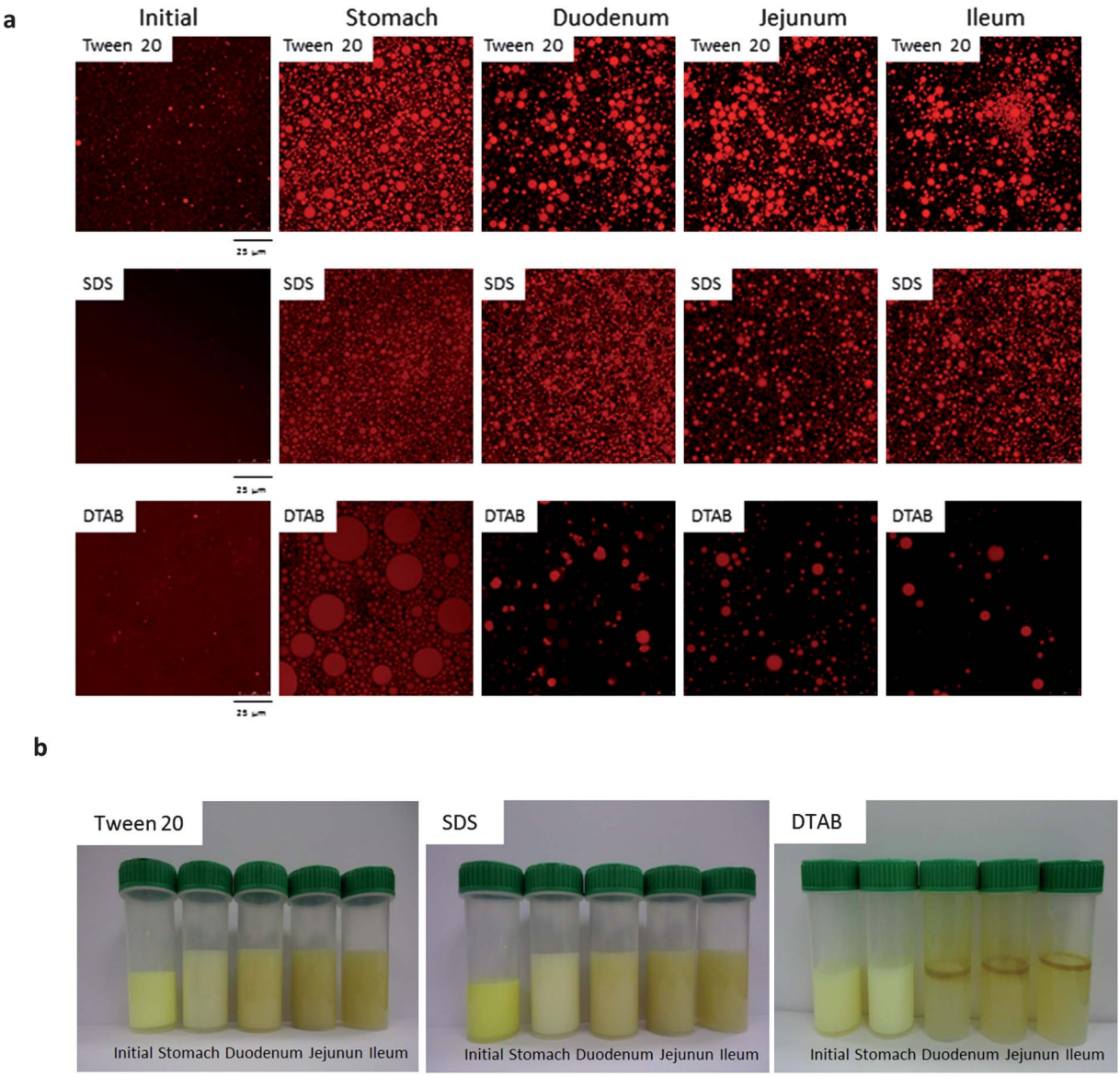

Fig. 3 Confocal images (a) and visual appearance of the samples (b) of curcumin nanoemulsions stabilized by different emulsifiers (Tween 20, SDS and DTAB) as they pass through an *in vitro* digestion model. The scale bar for all confocal images is 25 μm.

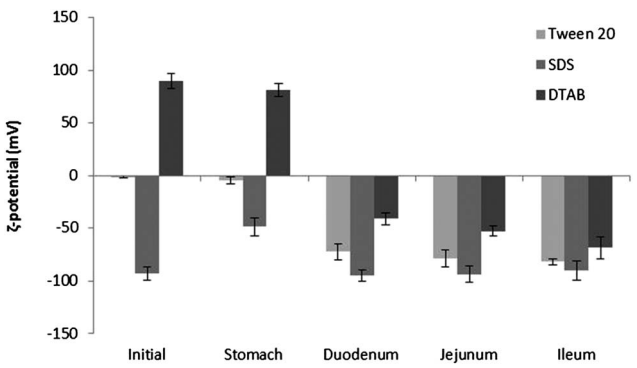

Fig. 4 ζ-potential values of curcumin nanoemulsions stabilized by different emulsifiers (Tween 20, SDS and DTAB) as they pass through an *in vitro* digestion model.

nanoemulsions. However, in the case of the SDS-stabilized nanoemulsions, the electrical charge became less negative. The pK_a of SDS is about 1.9;[27] therefore, as the environment of emulsions became more acidic, more SDS molecules are in the non-ionic state.

The addition of the simulated intestinal fluids resulted in all emulsions having a net negative charge. This led to a reversal of charge for the DTAB-stabilized nanoemulsions from positive to negative and the Tween 20-stabilized nanoemulsion gained a further increase in negative charge. The observed change in electrical charge can be attributed to the adsorption of anionic components present in the intestinal juices (*e.g.* bile salts) or the presence of free fatty acids (anionic), which are surface-active products of lipolysis. Bile salts are anionic bio-surfactants with a high affinity for the oil–water interface and are capable of

displacing surface-active compounds from an oil–water interface.[21,26,28] Bile salts then remove the digestion products from the interface and solubilize into the bulk aqueous phase.[25,28,29] Although a precise mechanism is difficult to define from the current measurements, the high negative charge reported for a DTAB-stabilized emulsions after digestion could be a result of the presence of bile salts at the interface or the digestion products of TAG (*i.e.* mono and diglycerides). These data are in agreement with previous work that has shown that the charge of emulsions stabilized by Tween 20, lysolecithin, caseinate and whey protein became more negative when they moved from a simulated stomach to a small intestine environment.[21]

At the end of the simulated digestion (ileum), the ζ-potential values of all the emulsions were fairly similar irrespective of the initial droplet charge.

3.4 *In vitro* digestibility

A measure of digestibility is the production of free fatty acids (FFA). Fig. 5 shows the results for the production of FFA during the simulated intestinal digestion of curcumin nanoemulsions stabilized by different emulsifiers.

The total FFA produced as measured from the back titration was the greatest for the Tween 20-stabilized emulsion. This increased production is attributed to the reduced size of the emulsion droplet (observed throughout simulated digestion) which maintains a large surface area for the binding of lipase and bile salts.

Emulsions stabilized with SDS and DTAB showed a reduced amount of FFA production in comparison to Tween 20. With the SDS-stabilized emulsion, charge repulsion could be preventing effective binding of bile salts and thus the binding of lipase was not being promoted. In this case the further increase in negative charge observed in the simulated small-intestine (Fig. 4) could have been mainly due to the presence of free fatty acids and not due to the effective binding of bile salts. In the case of the DTAB-stabilized emulsion, a clear phase separation (as seen in Fig. 3b) led to a significant reduction in surface area for enzyme binding, decreasing the rate of FFA production. Another explanation presented in the literature is the binding of FFA to DTAB altering the extent of digestion.[30] For all three emulsifier types, FFA production equilibrium was reached. This constant value could be attributed to the inhibition of lipase activity by the FFA released.[9] Our observations suggest that the size of the emulsion droplets as well as the emulsifier surface charge affected the total production of FFA.

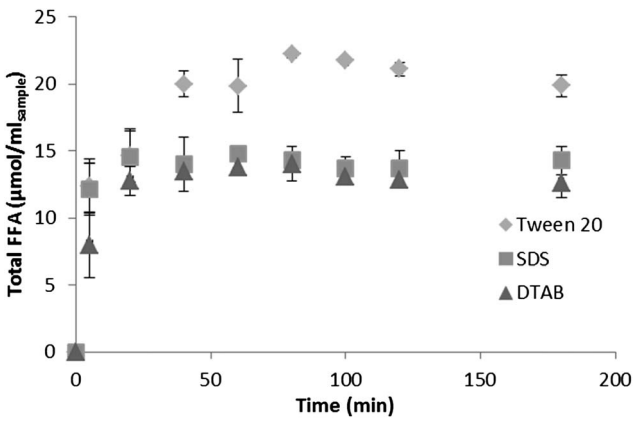

Fig. 5 Influence of emulsifier type on the production of total free fatty acids from curcumin nanoemulsions.

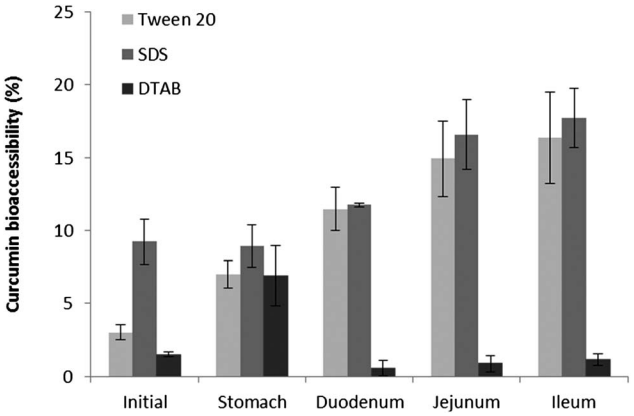

Fig. 6 Effect of initial emulsifier type on curcumin bioavailability as nanoemulsions pass through an *in vitro* digestion model.

3.5 *In vitro* curcumin bioavailability

The influence of the emulsifier type on the bioavailability of curcumin at different stages of the simulated digestion process is presented in Fig. 6.

The bioavailability of curcumin, measured as the curcumin concentration in the mixed micelle phase, depends on the emulsifier type and on the digestion stage. The curcumin bioavailability for nanoemulsions stabilized by Tween 20 increased with digestion time and appears to have significance only for SDS-stabilized emulsion in the jejunum and ileum. This behaviour can be attributed to the formation of digestion products that have the ability to form mixed micelles capable of solubilizing highly lipophilic components. Also, the greater free fatty acid production observed in the case of Tween 20-stabilized nanoemulsions (Fig. 5) could explain the high curcumin bioavailability (in relation to the initial bioavailability) obtained for the Tween 20-stabilized nanoemulsion.

In contrast, curcumin had very low bioavailability under simulated intestinal conditions when it was encapsulated in an emulsion containing DTAB. This effect can be attributed to the fact that under simulated intestinal conditions, DTAB-stabilized emulsions are highly unstable, leading to phase separation. Curcumin, which is soluble only in the oil phase, will have remained in the separated bulk oil, and with this reduced surface area, the digestive enzymes will not have acted to enable mixed micelle formation, thus reducing bioavailability. Similar results were obtained in other work, in which it was observed that the total amount of β-carotene present in the micellar phase during each stage of digestion is much higher in small-sized emulsions compared to emulsions that are larger in size; this is due to the increased surface area for enzyme interaction.[31]

4 Conclusions

A digestion model involving the *in vitro* simulation of stomach, duodenum, jejunum and ileum was used to evaluate the impact of surface charge on the digestion of the curcumin nanoemulsions. Although all the nanoemulsions tested were markedly affected by the digestion process, the DTAB-stabilized emulsions showed the most drastic change in the droplet size and electrical charge during digestion. The positively charged surface of DTAB-stabilized nanoemulsions could have promoted the adsorption of anionic lipase and anionic bile salts to the oil–water interface; however, the reduction in surface area would not have promoted enzyme binding to the emulsion interface. The initial emulsifier was also found to impact curcumin bioavailability due to the differences in the formation of digestion products that have the ability to form mixed micelles capable of solubilizing highly lipophilic components. Curcumin exhibited a very low bioavailability under intestinal conditions in the presence of DTAB as emulsifier. The higher curcumin bioavailability observed for Tween 20-stabilized nanoemulsions (in relation to the initial bioavailability) could be related to the greater free fatty acid production obtained for this nanoemulsion as a direct result of the emulsion droplet size.

The results from this work showed that the behaviour of nanoemulsions (*e.g.* free fatty acids release and bioavailability of the bioactive compound incorporated) during *in vitro* digestion depends on the charge of the initial emulsifier. This work also highlighted the importance of using a more realistic digestion model, particularly of subjecting the emulsions to the simulated gastric environment, once changes in pH, ionic strength, the gastric enzymes activity and shear impact the emulsion properties in the small-intestine. The obtained results will contribute to the development of optimized nanoemulsion-based delivery systems to protect and release bioactive lipophilic compounds within the human body, for food and pharmaceutical applications.

Acknowledgements

Ana C. Pinheiro and Hélder Silva gratefully acknowledge the Fundação para a Ciência e Tecnologia (FCT, Portugal) for their fellowships (SFRH/BD/48120/2008 and SFRH/BD/81288/2011 respectively). The author Ana C. Pinheiro would also like to acknowledge the European Union, through Cost Action FA1001 and the author Manuel A. Coimbra gratefully acknowledges QOPNA (project PEst-C/QUI/UI0062/2011).

References

1 Y.-F. Wang, J.-J. Shao, C.-H. Zhou, D.-L. Zhang, X.-M. Bie, F.-X. Lv, C. Zhang and Z.-X. Lu, *Food Control*, 2012, **27**, 113–117.
2 O. P. Sharma, *Biochem. Pharmacol.*, 1976, **25**, 1811–1812.
3 Y. Wang, Z. Lu, H. Wu and F. Lv, *Int. J. Food Microbiol.*, 2009, **136**, 71–74.
4 R. C. Srimal and B. N. Dhawan, *J. Pharm. Pharmacol.*, 1973, **25**, 447–452.
5 G. S. Sidhu, A. K. Singh, D. Thaloor, K. K. Banaudha, G. K. Patnaik, R. C. Srimal and R. K. Maheshwari, *Wound Repair Regen.*, 1998, **6**, 167–177.
6 R. Kuttan, P. Bhanumathy, K. Nirmala and M. C. George, *Cancer Lett.*, 1985, **29**, 197–202.
7 P. Anand, A. B. Kunnumakkara, R. A. Newman and B. B. Aggarwal, *Mol. Pharmacol.*, 2007, **4**, 807–818.
8 K. Ahmed, Y. Li, D. J. McClements and H. Xiao, *Food Chem.*, 2012, **132**, 799–807.
9 H. Silva, M. Cerqueira and A. Vicente, *Food Bioprocess Technol.*, 2012, **5**, 854–867.
10 Y. Pafumi, D. Lairon, P. L. de la Porte, C. Juhel, J. Storch, M. Hamosh and M. Armand, *J. Biol. Chem.*, 2002, **277**, 28070–28079.
11 D. J. McClements and H. Xiao, *Food Funct.*, 2012, **3**, 202–220.
12 S. Rozner, D. E. Shalev, A. I. Shames, M. F. Ottaviani, A. Aserin and N. Garti, *Colloids Surf., B*, 2010, **77**, 22–30.
13 Y. Li and D. J. McClements, *J. Agric. Food Chem.*, 2010, **58**, 8085–8092.
14 M. Vardakou, A. Mercuri, S. Barker, D. Craig, R. Faulks and M. Wickham, *AAPS PharmSciTech*, 2011, **12**, 620–626.
15 P. Reis, T. Raab, J. Chuat, M. Leser, R. Miller, H. Watzke and K. Holmberg, *Food Biophys.*, 2008, **3**, 370–381.
16 F. Kong and R. P. Singh, *J. Food Sci.*, 2010, **75**, E627–E635.
17 Y. Li, M. Hu and D. J. McClements, *Food Chem.*, 2011, **126**, 498–505.
18 E. Troncoso, J. M. Aguilera and D. J. McClements, *Food Hydrocolloids*, 2012, **27**, 355–363.
19 U. Lesmes, P. Baudot and D. J. McClements, *J. Agric. Food Chem.*, 2010, **58**, 7962–7969.
20 A. Sarkar, K. K. T. Goh, R. P. Singh and H. Singh, *Food Hydrocolloids*, 2009, **23**, 1563–1569.
21 S. J. Hur, E. A. Decker and D. J. McClements, *Food Chem.*, 2009, **114**, 253–262.
22 A. Helbig, E. Silletti, E. Timmerman, R. J. Hamer and H. Gruppen, *Food Hydrocolloids*, 2012, **28**, 10–19.
23 S. Amara, D. Lafont, B. Fiorentino, P. Boullanger, F. Carrière and A. De Caro, *Biochim.Biophys. Acta, Mol. Cell Biol. Lipids*, 2009, **1791**, 983–990.
24 P. Pinsirodom and K. L. Parkin, in *Current Protocols in Food Analytical Chemistry*, John Wiley & Sons, Inc., 2001.
25 M. Golding, T. J. Wooster, L. Day, M. Xu, L. Lundin, J. Keogh and P. Clifton, *Soft Matter*, 2011, **7**, 3513–3523.
26 S. Mun, E. A. Decker and D. J. McClements, *Food Res. Int.*, 2007, **40**, 770–781.
27 S. Chakraborty, D. Shukla, A. Jain, B. Mishra and S. Singh, *J. Colloid Interface Sci.*, 2009, **335**, 242–249.
28 J. Maldonado-Valderrama, N. C. Woodward, A. P. Gunning, M. J. Ridout, F. A. Husband, A. R. Mackie, V. J. Morris and P. J. Wilde, *Langmuir*, 2008, **24**, 6759–6767.
29 A. Malaki Nik, A. J. Wright and M. Corredig, *Colloids Surf., B*, 2011, **83**, 321–330.
30 A. Dahan and A. Hoffman, *Pharm. Res.*, 2006, **23**, 2165–2174.
31 Y. Liu, Z. Hou, F. Lei, Y. Chang and Y. Gao, *Innovative Food Sci. Emerging Technol.*, 2012, **15**, 86–95.

